DALAT UNIVERSITY JOURNAL OF SCIENCE Volume 14, Issue 3S, 2024 17–29

RECONSTRUCTION OF DIVACANCY IN ZIGZAG-BUCKLED SILICENE NANORIBBONS

Ngo Van Chinh[a], Pham Nguyen Huu Hanh[a], Nguyen Thi Kim Quyen[a, b], Phan Thi Kim Loan[c*], Vu Thanh Tra[c, d*]

[a]Graduate School, College of Natural Sciences, Can Tho University, Can Tho, Vietnam
[b]Faculty of Engineering – Technology, Kien Giang University, Kien Giang, Vietnam
[c]Department of Physics, School of Education, Can Tho University, Can Tho, Vietnam
[d]College of Science, Department of Electrophysics, National Yangming Chiaotung University, Taiwan
[*]Corresponding author: Email: vttra@ctu.edu.vn

Article history
Received: September 14th, 2023
Received in revised form: November 4th, 2023 | Accepted: November 27th, 2023
Available online: March 13th, 2024

Abstract

In this study, we use a tight binding model to investigate structural and electronic changes in zigzag-buckled silicene nanoribbons (*ZBSiNRs*) *with two vacancies at different positions. We divide the defects into two categories based on a difference in geometric properties. The results show that the first- and second-order interaction parameters of two atoms of the same type play an important role in the electronic properties of this material. Vacancies near the edge have a stronger effect than those near the center of the ribbons. We further show that each type of divacancy will give a different result under the influence of a perpendicular electric field. This is a favorable condition for controlling the conductive state of materials in future applications in the semiconductor and thermoelectric industries.*

Keywords: Buckled silicene nanoribbons; Divacancy; Electric field; Electronic structure; Tight binding.

DOI: http://doi.org/10.37569/DalatUniversity.14.3S.1232(2024)

Article type: (peer-reviewed) Full-length research article

1. INTRODUCTION

Silicene, a material with an energy band structure at the Fermi level similar to graphene, has attracted much attention from scientists (Castro Neto et al., 2009; Novoselov et al., 2004, 2005). The similarity in the energy band structure is leading to potential applications of this material in practical fields (Guzmán-Verri & Lew Yan Voon, 2007; Vogt et al., 2012). In addition to the planar state, silicene also exists in a stable warped state known as buckled silicene (Cahangirov et al., 2009; Sahin et al., 2009; Zhang et al., 2012). This warped state has graphene-like properties and allows the band gap to be changed for applications in electronic semiconductor devices (Molle et al., 2018; Nguyen et al., 2021; Peng et al., 2020; Sivek et al., 2013; Zhang et al., 2017; Zhu & Schwingenschlögl, 2016).

Defects in a certain range will bring about many interesting changes in the structure and properties of materials (Li et al., 2015). In particular, the doping of atoms through adatoms and substitutions leads to many interesting changes in the electronic and magnetic properties of materials (Biel et al., 2009; Ersan et al., 2014; Guo et al., 2017; Huynh et al., 2021). If defects exist as zero-dimensional point defects, typically including Stone-Wales (STW), vacancy, and divacancy (DV) defects, the mechanical properties of the material are altered (Botello-Mendez et al., 2011; Le & Nguyen, 2015; Manjanath & Singh, 2014; Mortazavi & Ahzi, 2013; Sahin et al., 2013). However, they offer a scalability band gap, leading to a significant change in the thermal conductivity of the material (An et al., 2014; Shirodkar & Waghmare, 2012). In particular, some studies using density functional theory (DFT) calculations have predicted that when the number of vacancy units is 10 or more, it is energetically favorable for a single-row arrangement of atoms to form new structures (Ghosh et al., 2015; Kim et al., 2013). With the two missing atoms, the reconstruction will introduce many different types of reconstructions. However, recent experimental studies have shown that when restructuring occurs, the 5–8–5 structure is the most stable and may also bring about many new properties. It has also been shown using simulation methods and theoretical calculations that new bonds will be created around the removed bonds in the 5–8–5 model. In particular, this model shows suitability given that the new restructuring parameters have interaction parameter values equivalent to those of the old bonds, thus ensuring the sustainability of the material. In a previous study by Ngo et al. (2023), we only had the opportunity to present the effect of divacancy on two adjacent obliquely bonded atoms (type 1). Nevertheless, we predict that if divacancy occurs with two atoms bonded in a straight line parallel to the width of the nanoribbon (type 2), it will also yield interesting results. Therefore, in this article, we examine restructuring for type 2 divacancy and compare the effects of both types of divacancy to provide a general picture of the effects of divacancy combined with restructuring on the properties of zigzag-buckled silicene nanoribbons (ZBSiNRs).

2. MODEL AND CALCULATION METHOD

2.1. Model

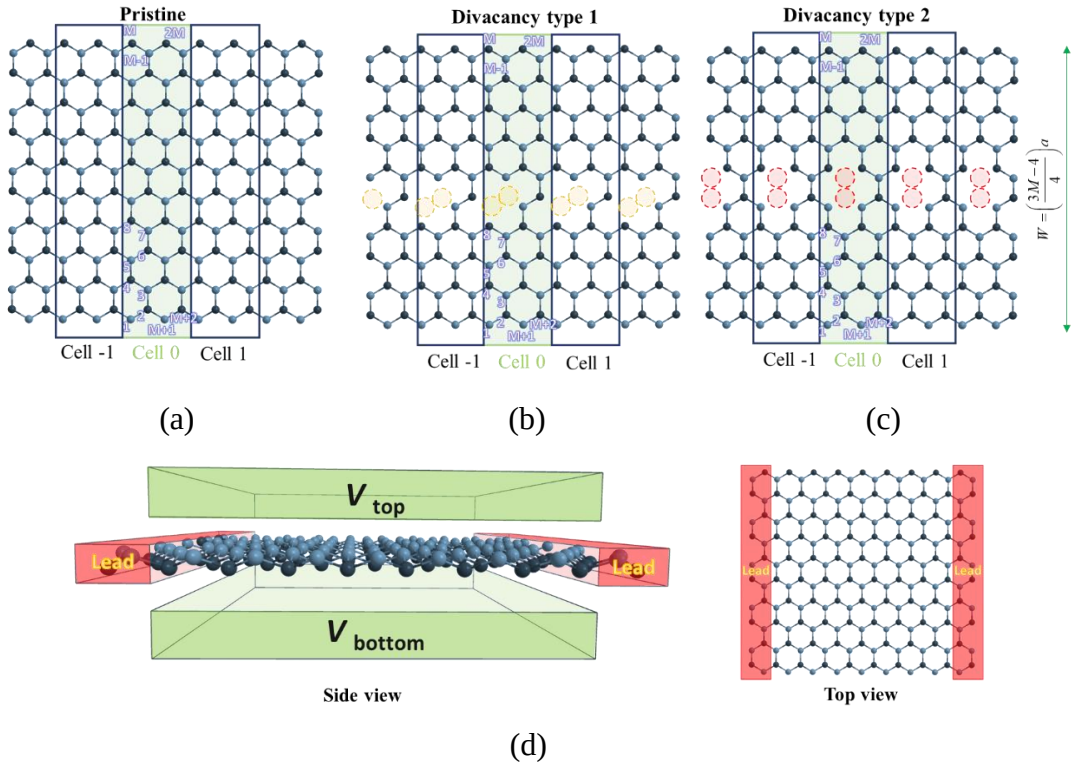

Figure 1. Atomic structure of ZBSiNRs with divacancies

Notes: (a) Pristine structure; (b) Type 1 divacancy structure; (c) Type 2 divacancy structure; (d) Model representation for the case of an electric field applied at the top and bottom gates.

In Figure 1, we investigate the structure of ZBSiNRs with and without defects. We begin with a perfect silicene nanoribbon of width W (Figure 1a). The ZBSiNRs are composed of alternating bonds between sp^2- and sp^3-hybridized silicene atoms to form a honeycomb structure with an interatomic distance of $a = 0.224\ nm$. In particular, such a structure forms a warped structure with distance $d = 0.044\ nm$ between the upper layer atoms with sp^3 hybridization and lower layer atoms with sp^2 hybridization. We investigate material with width $W = \left(\frac{3M-4}{4}\right)a$ where M is the number of atoms in a zigzag line that spans the width of the material. In particular, we investigate materials with $W = 6.832$ nm, corresponding to $M = 42$. Then, we form divacancy defects by directly removing atoms from the perfect (pristine) silicene nanoribbon. We remove bonds for the atoms at the divacancy and perform computations that enhance refactoring to form new structures. In the type 1 defect structure (Figure 1b), two adjacent atoms that are obliquely bonded are removed, such as pairs of atoms at positions 5–6 and 9–10. In the type 2 defect structure (Figure 1c), the two removed atoms are two adjacent atoms bonded in a straight line, such as atoms at positions 6–7 and 10–11. The differences in geometry lead to differences in the restructuring of each type of material.

In addition, to investigate the sensitivity of the electric field in controlling the band gap of buckled silicene (Khoeini & Jafarkhani, 2019; Nguyen et al., 2021), we modeled the use of two electrodes, V_{top} and V_{bottom}, to apply an electric field to the reconstructed material, as shown in Figure 1d. We combined the reconstructed divacancy model with the perpendicular electric field and calculated based on the tight binding approximation.

2.2. Calculation method

To investigate the energy bands of the material, we chose to calculate by the tight binding method with the Hamiltonian in Equation (1) (Cresti et al., 2008):

$$H = -\sum_{k=0}^{6} t_k \sum_{\langle ij \rangle} \left(|i\rangle\langle j| + |j\rangle\langle i| \right) + \sum_i \left(\varepsilon_i + (-1)^i \Delta \right) |i\rangle\langle i| + q \frac{V_t}{2} \sum_i (-1)^i |i\rangle\langle i| \qquad (1)$$

- The first term represents the interaction energy between the atoms. For the pristine case, we only investigate the nearest neighbor interaction with t_0 = 1.6 eV (Abdelsalam et al., 2015). For the defect structures, we extend the calculations to the next nearest neighbor interactions between the dissociated and defect atoms using new interaction parameters.

- The second term characterizes the warping of the material sheet. The internal energy difference between the two types of sp^2 and sp^3 hybrid atoms is expressed by the parameter Δ (Peng et al., 2013), the parameter ε indicates onsite energy

- The third term characterizes the amount of energy supplied to the material in the presence of an electric field, where q represents the charge of the electron and V_t represents the voltage value applied to create the electric field (Nguyen et al., 2021).

For convenience of calculation, we divide the ZBSiNR into unit cells. The atoms in a unit cell are numbered from 1 to 2M, corresponding to two zigzag lines in a cell (Figure 1a). We then use the matrix form to represent the Hamiltonian in Equation (1) as follows:

- The first term is represented by the interaction matrices H_{00}, H_{01}, and $H_{0\text{-}1}$, which correspond to the interactions between neighboring cells.

$$H_{00} = \begin{bmatrix} h_{11} & h_{12} \\ h_{21} & h_{22} \end{bmatrix}_{(2M \times 2M)}; H_{01} = \begin{bmatrix} l_{11} & l_{12} \\ l_{21} & l_{22} \end{bmatrix}_{(2M \times 2M)}; H_{0-1} = \begin{bmatrix} p_{11} & p_{12} \\ p_{21} & p_{22} \end{bmatrix}_{(2M \times 2M)} \qquad (2)$$

where

- h_{ij} represents the interaction energy between the *i-th* and *j-th* zigzag lines of cell 0 $(i, j \in M)$;

- l_{ij} represents the interaction energy between the *i-th* zigzag line of cell 0 and the *j-th* zigzag line of cell 1 $\left(i,\ j \in M\right)$;

- p_{ij} represents the interaction energy between the *i-th* zigzag line of cell 0 and the *j-th* zigzag line of cell -1 $\left(i,\ j \in M\right)$.

- The second term of Equation (1) is represented by the principal diagonal matrix representing the difference between the sp^2 and sp^3 atoms:

$$H_B = \begin{bmatrix} \varepsilon+\Delta & 0 & \cdots & 0 & 0 \\ 0 & \varepsilon-\Delta & \cdots & 0 & 0 \\ \vdots & \vdots & \ddots & \vdots & \vdots \\ 0 & 0 & \cdots & \varepsilon+\Delta & 0 \\ 0 & 0 & \cdots & 0 & \varepsilon-\Delta \end{bmatrix}_{(2M\times 2M)} . \quad (3)$$

- The third term of Equation (1) is the energy added to each atom, so it has the following form:

$$U_{\text{ext}} = q\begin{bmatrix} -\frac{V_t}{2} & 0 & \cdots & 0 & 0 \\ 0 & \frac{V_t}{2} & \cdots & 0 & 0 \\ \vdots & \vdots & \ddots & \vdots & \vdots \\ 0 & 0 & \cdots & -\frac{V_t}{2} & 0 \\ 0 & 0 & \cdots & 0 & \frac{V_t}{2} \end{bmatrix}_{(2M\times 2M)} . \quad (4)$$

The Hamiltonian of Equation (1) can be rewritten with matrices H_{00}, H_{01}, $H_{0\text{-}1}$, H_{B}, and U_{ext} as

$$H = H_{00} + H_{01}\exp\left(i\vec{k}_x\vec{R}_{01}\right) + H_{0-1}\exp\left(i\vec{k}_x\vec{R}_{0-1}\right) + H_B + U_{\text{ext}} . \quad (5)$$

3. RESULTS AND DISCUSSION

3.1. Reconstruction according to the 5–8–5 model with type 1 divacancy

Four atoms will lose their bonds for type 1 divacancy (Figure 1b), and we will build new quadratic interactions, namely, t_2, t_3, t_4, t_5, and t_6, as shown in Figure 2a. Based on the stability of the material, the removal of two atoms from a cell will lead to the dissociation of four atoms. To ensure the stability of this structure, the atoms that have lost their bonds tend to bond together, as indicated by the t_4 and t_5 interactions (Figure 2a). This shift also affects other atoms, changing the t_1, t_2, t_3, and t_6 interactions. To investigate the regeneration of the material, we calibrated the interaction parameters on

the basis of the experimental model combined with the theory of the Coulomb interaction potential field (Li et al., 2015; Piraux et al., 2021). We provide a model to predict the recombination as shown in Figure 2b with the parameters given in Table 1. Such a reconstruction is called a silicene defect 5–8–5 (Botello-Mendez et al., 2011; Li et al., 2015).

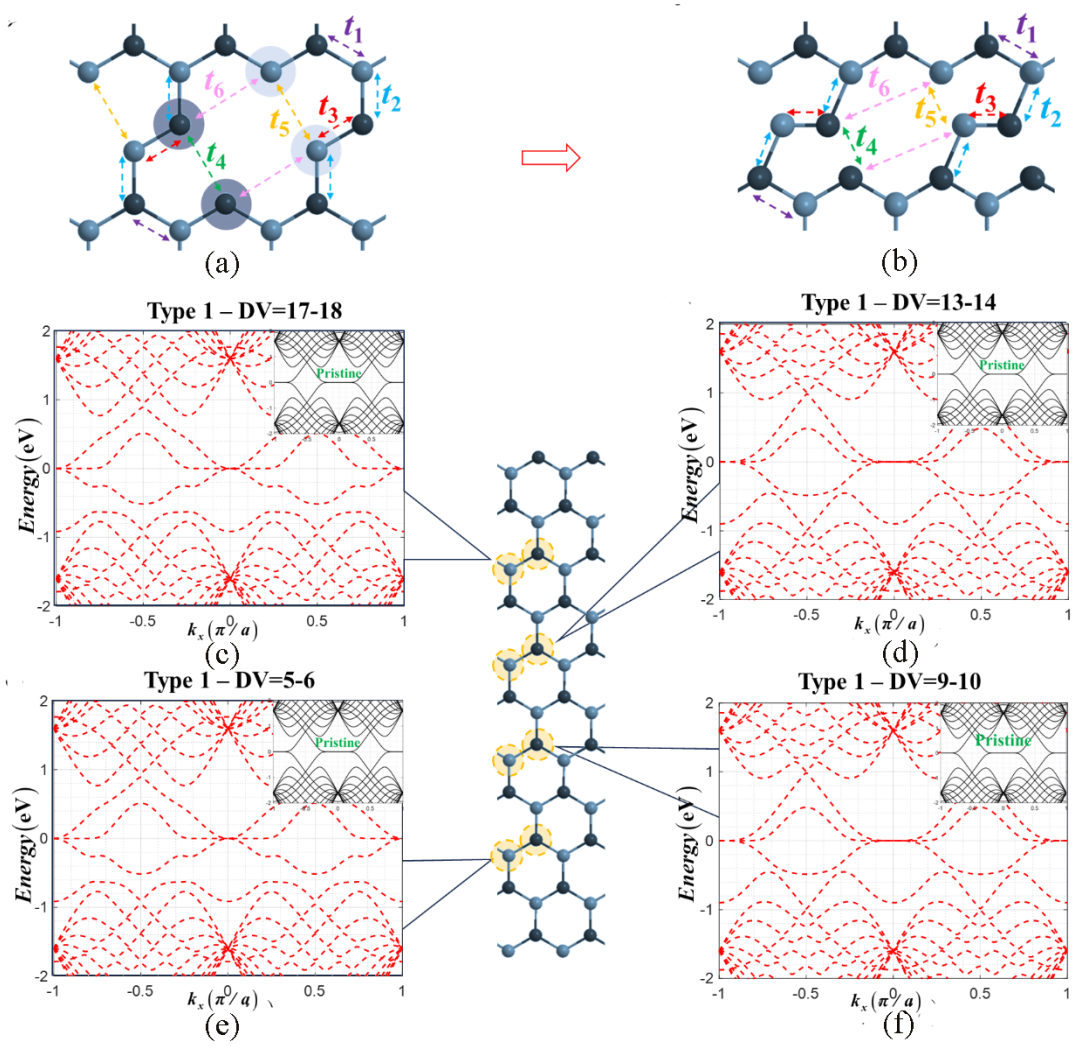

Figure 2. Reconstruction according to the 5–8–5 model

Notes: (a-b) Change in interaction parameters during refactoring; (c-f) Influence of the divacancy (DV) position on the energy band structure.

Table 1. Interaction parameters with reconstruction according to the 5–8–5 model

Parameter	t_1	t_2	t_3	t_4	t_5	t_6
Distance (nm)	0.224	0.224	0.224	0.224	0.224	0.672
Energy (eV)	-1.6	t_1	t_1	t_1	t_1	0

Next, we created a type 1 divacancy at various locations to investigate the influence of defects on the band structure of this material. Specifically, we created defects

at positions 17–18, 13–14, 9–10, and 5–6. Under the influence of the reconstruction, the atoms will form a new structure with 5–8–5 rings at different positions based on the defect location. The energy bands are significantly affected by the transformation of the energy curves around the Fermi level, as shown in Figure 2(c-f). The energy bands show up to three lines close to the Fermi level, rapidly decreasing the flatband length. Therefore, the results indicate that the material properties have strongly changed, especially for conductivity. By comparing the simultaneous effect of each defect location, we found that the effect is greater when the defects appear closer to the material boundary. This is completely consistent with the results of previous studies on the properties of zigzag boundaries (Fujita et al., 1996).

Although the band gap remains close to zero, the band structure exhibits a significant change in electron arrangement. The appearance of an additional line around the Fermi level indicates that the increase in electronic excitation channels depends on the defect. According to previous studies (e.g. Nguyen et al., 2021), it is possible to control the band gap based on the effect of an electric field on silicene. Therefore, tuning the excitation channels based on the atomic vacancy in combination with the presence of an electric field will be of great significance in modulating the conductivity of materials. The interesting changes observed when a perpendicular electric field is introduced will be explained in detail in Sub-section 3.3.

3.2. Reconstruction according to the d5d7 model with type 2 divacancy

Similar to the construction of the type 1 divacancy defect model, we simulate the changes in the hopping parameters of the type 2 divacancy defect model with new quadratic interactions: t'_1, t'_2, t'_3, t'_4, t'_5, and t'_6 (Figure 3a). We use the same reasoning as with the 5–8–5 model to reconstruct this model; however, instead of being able to form stable 5–8–5 rings, as in the type 1 divacancy, the difference in geometry means that the 5–8–5 rings are unstable for the type 2 divacancy (Figure 3b). The restructuring leads to the displacement of atoms, which corresponds to the appearance of weak bonds t'_3 when the distance between atoms is quite large. Moreover, it is easy to see that the interaction angle between atoms connected by t'_2 and t'_3 is unstable (Figure 3b). To form a stable reconstruction, we add the STW defect (rotate the Si-Si bond by 90°) (Botello-Mendez et al., 2011). Two atoms connected vertically by a t'_6 interaction in ring 8 will rotate by 90° to form a horizontal interaction (Figure 3c).

A structure consisting of bonds 5–7, known as d5d7 (double 5 double 7), results from the combination of a divacancy and the STW defect (Figure 3c) (Botello-Mendez et al., 2011; Li et al., 2015). The d5d7 structure ensures the geometric stability of the material after reconstruction, with the distance between the atoms being not too different, and creates a new geometry with stable pentagons and heptagons. Based on the success in adjusting the parameters in the previous model, we also rely on the Coulomb interaction theory and experimental results to adjust the interaction parameters to determine the energy band structure of the material. We provide a model (Figure 3c) for predicting the recombination generated with the parameters given in Table 2.

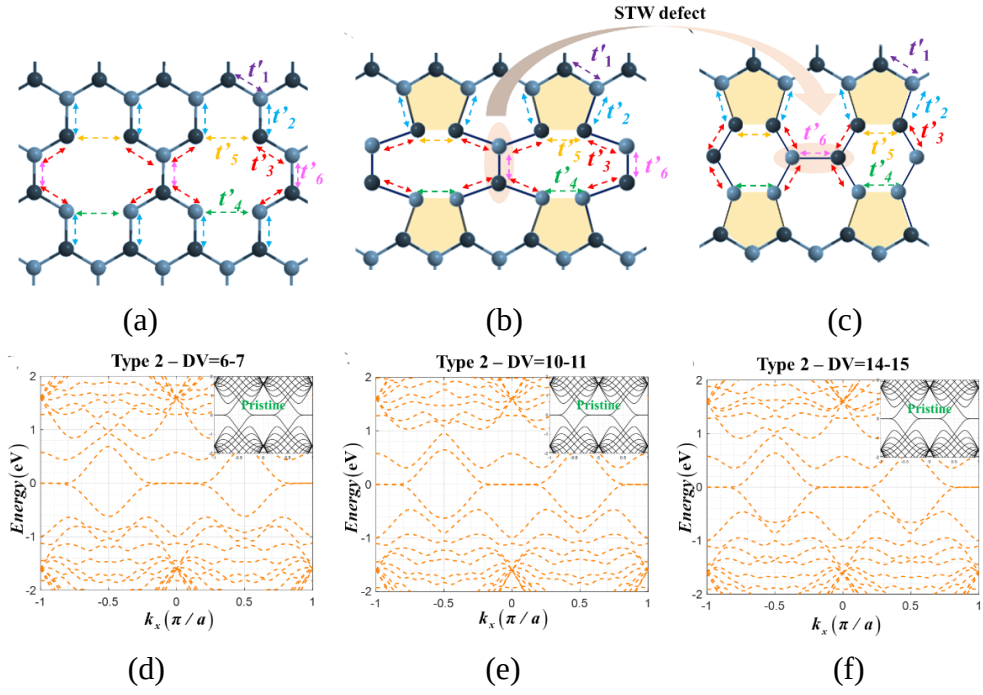

Figure 3. Reconstruction according to the d5d7 model

Notes: (a-c) Change in interaction parameters during refactoring; (d-f) Influence of the divacancy (DV) position on the energy band structure.

Table 2. Interaction parameters with reconstruction according to the d5d7 model

Parameter	t'_1	t'_2	t'_3	t'_4	t'_5	t'_6
Distance (nm)	0.224	0.224	0.224	0.224	0.224	0.672
Energy(eV)	-1.6	t_1	t_1	t_1	t_1	0

The energy band structure of the d5d7 model is shown in Figure 3d to Figure 3f. The reconstruction retains the band gap characteristic of the ZBSiNRs. The band structure retains symmetry, and the band gap remains almost zero near the Fermi level. The effect of the defect will be evident as more energy levels are examined further from the Fermi level. In particular, the second energy levels of the conduction and valence bands have changed significantly. For the defect-free structure at $k_x = 0$, electrons are concentrated at energies of 1.6 eV for the conduction band and -1.6 eV for the valence band. When there is a defect and reconstruction, electrons are concentrated at energies of 0.6 eV and -1.0 eV in the conduction and valence bands, respectively. Moreover, the influence of defect position near the edge and in the center of the material is not obvious because of the formation of rings 5–7 compared to ring 6, which is relatively stable.

By examining the energy band structure of the two types of divacancy, we realized that there are significant changes in the material properties. Although divacancy does not affect the band gap much, the shape and number of energy lines change markedly. This indicates that the defect strongly influences the formation of excited states around the

Fermi level, increasing the number of electron transfer channels for ZBSiNR materials. Therefore, we show in the next section that applying an electric field takes advantage of the potential for multiple excitation channels of defects (compared with pristine materials) to control the material's band gap.

3.3. Impact of an electric field

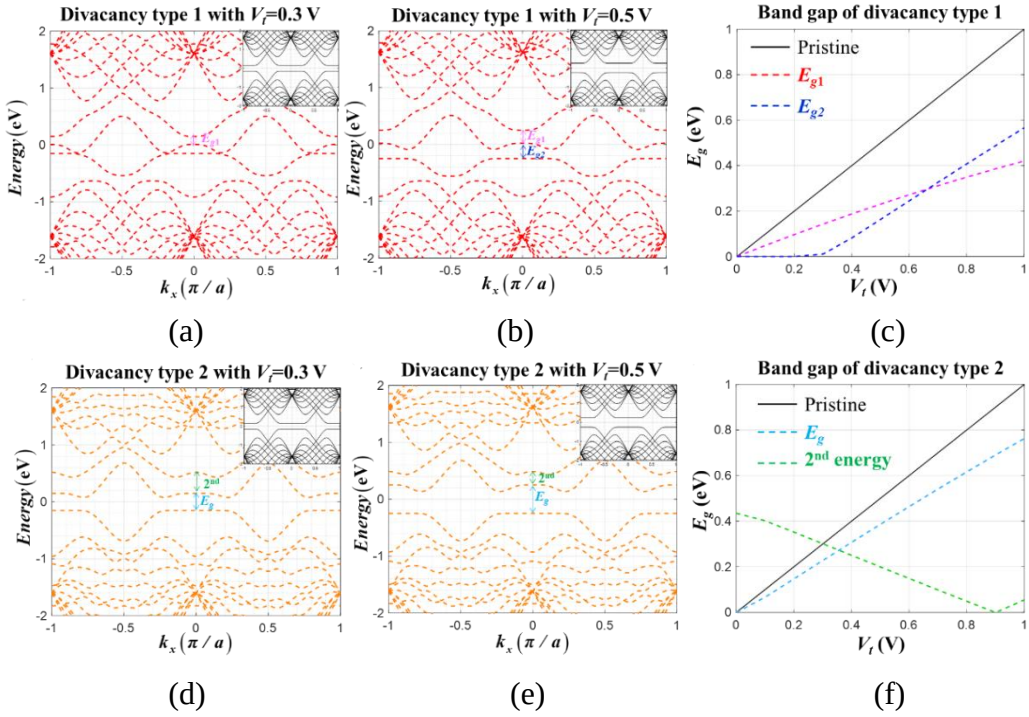

Figure 4. Impact of an electric field on the electronic properties

Notes: (a-c) Type 1 divacancy; (d-f) Type 2 divacancy.

The gap size of this material can be controlled by applying a perpendicular electric field (Figure 4). When the electric field is applied, the electrons in the two layers receive different amounts of energy. The atoms in the upper layer receive an energy of $qV_t/2$, whereas the atoms in the lower layer receive an energy of $-qV_t/2$. This leads to energy level separation, pushing the energy levels to both sides of the Fermi level and forming a band gap. To investigate the simultaneous influence of defects and the electric field, we chose locations where the defect impact is greatest, particularly at DV = 5–6 and DV = 6–7 for type 1 and type 2 divacancies, respectively.

The electric field separates the energy lines around the Fermi level into three separate paths for type 1 divacancy, as shown in Figure 4a and 4b. One line remains close to the Fermi level, and the other two are pushed to either side of the conduction and valence bands, similar to the perfect structure. This shift in energy levels can be explained by the fact that the electrons attached to the defective atom will return to the ground state around the Fermi level, and these electrons will again be located in the region of the canceled electric field, causing the electric field to have little effect on this energy curve

compared to the other two energy lines. In particular, when using an electric field of small magnitude, separating the energy levels creates a valid band gap of 0.143 eV (Figure 4a). However, when using an electric field of greater intensity, this shift creates two band gaps, which increases the number of electronic excitation channels. Specifically, with a voltage of 0.5 V, the E_{g1} and E_{g2} values are 0.230 eV and 0.163 eV, respectively (Figure 4b). We obtained interesting results when simultaneously investigating the E_{g1} and E_{g2} values according to the applied potential, as shown in Figure 4c. E_{g2} only makes sense when the voltage used is 0.3 V. In particular, above 0.7 V, E_{g2} has a stronger change than E_{g1}.

In the type 2 divacancy structure, the electric field strongly affects the two energy levels adjacent to the Fermi level, forming band gaps of 0.227 eV and 0.386 eV for potential values of 0.3. V and 0.5 V, respectively (Figure 4d to Figure 4e). However, the difference lies in that the second-order energy level is close to the first-order energy level. The energy gap is approximately 0.435 eV in the absence of an electric field, whereas in the presence of an electric field, the energy gap is 0.274 eV for V_t = 0.3 V and 0.200 eV for V_t = 0.5 V. This result facilitates an increase in the number of electron transfer channels. Moreover, the gap increases linearly with an increase in the electric field strength (Figure 4f). At the same time, the second energy line is pushed closer and closer to the first energy line.

In addition, when comparing the band gap between the two types of divacancy according to the electric field strength, we found that the band gap of the two materials increased linearly with the applied potential strength. However, the sensitivity of type 1 is lower than that of type 2, and the perfect structure has the greatest sensitivity. Therefore, the electric field can both widen the band gap of the material and provide control over other excitation channels. This is significant in various applications of electric fields to materials containing defects.

4. CONCLUSION

Through theoretical calculations based on experiments, we have successfully built a set of reconstruction parameters for DV materials. The band structure changed markedly with the reconstruction, although the band gap is still almost zero. However, the type 1 divacancy structure has an additional energy line near the Fermi level, whereas the type 2 divacancy structure creates an energy line near the Fermi level, providing more optical excitation and displacement channels. In addition, the effect is greater when defects and reconstructions occur near the edge. In particular, the electric field has great significance in expanding the band gap and adjusting the electronic excitation channels. For the type 1 structure, the electric field opens two sub-band gaps, in which each potential interval has a different meaning for each type of band gap. For the type 2 structure, the electric field also controls the electron transfer channels. This has huge potential for using a combination of external stimuli to create materials suitable for the evolving needs of materials science.

ACKNOWLEDGMENTS

This research was supported by the Vietnam National Foundation for Science and Technology Development (NAFOSTED) under grant number 103.10-2020.10.

REFERENCES

Abdelsalam, H., Espinosa-Ortega, T., & Lukyanchuk, I. (2015). Tuning of zero energy states in quantum dots of silicene and bilayer graphene by electric field. *Superlattices and Microstructures, 87*, 137–142. https://doi.org/10.1016/j.spmi.2015.04.038

An, R.-L., Wang, X.-F., Vasilopoulos, P., Liu, Y.-S., Chen, A.-B., Dong, Y.-J., & Zhai, M.-X. (2014). Vacancy effects on electric and thermoelectric properties of zigzag silicene nanoribbons. *Journal of Physical Chemistry C*, *118*(37), 21339–21346. https://doi.org/10.1021/jp506111a

Biel, B., Blase, X., Triozon, F., & Roche, S. (2009). Anomalous doping effects on charge transport in graphene nanoribbons. *Physical Review Letters*, *102*(9), 096803. https://doi.org/10.1103/PhysRevLett.102.096803

Botello-Mendez, A. R., Declerck, X., Terrones, M., Terronesa, H., & Charliera, J.-C. (2011). One-dimensional extended lines of divacancy defects in graphene. *Nanoscale, 3*, 2868–2872. https://doi.org/10.1039/C0NR00820F

Cahangirov, S., Topsakal, M., Aktürk, E., Şahin, H., & Ciraci, S. (2009). Two- and one-dimensional honeycomb structures of silicon and germanium. *Physical Review Letters*, *102*(23), 236804. https://doi.org/10.1103/PhysRevLett.102.236804

Castro Neto, A. H., Guinea, F., Peres, N. M. R., Novoselov, K. S., & Geim, A. K. (2009). The electronic properties of graphene. *Reviews of Modern Physics*, *81*(1), 109–162. https://doi.org/10.1103/RevModPhys.81.109

Cresti, A., Grosso, G., & Parravicini, G. P. (2008). Valley-valve effect and even-odd chain parity in p-n graphene junctions. *Physical Review B*, *77*(23), 233402. https://doi.org/10.1103/PhysRevB.77.233402

Ersan, F., Arslanalp, Ö., Gökoğlu, G., & Aktürk, E. (2014). Effects of silver adatoms on the electronic structure of silicene. *Applied Surface Science*, *311*, 9–13. https://doi.org/10.1016/j.apsusc.2014.04.176

Fujita, M., Wakabayashi, K., Nakada, K., & Kusakabe, K. (1996). Peculiar localized state at zigzag graphite edge. *Journal of the Physical Society of Japan*, *65*(7), 1920–1923. http://dx.doi.org/10.1143/JPSJ.65.1920

Ghosh, D., Parida, P., & Pati, S. K. (2015). Stable line defects in silicene. *Physical Review B*, *92*(19), 195136. https://doi.org/10.1103/PhysRevB.92.195136

Guo, G., Mao, Y., Zhong, J., Yuan, J., & Zhao, H. (2017). Design lithium storage materials by lithium adatoms adsorption at the edges of zigzag silicene nanoribbon: A first principle study. *Applied Surface Science*, *406*, 161–169. https://doi.org/10.1016/j.apsusc.2017.02.053

Guzmán-Verri, G. G., & Lew Yan Voon, L. C. (2007). Electronic structure of silicon-based nanostructures. *Physical Review B*, *76*(7), 075131. https://doi.org/10.1103/PhysRevB.76.075131

Huynh, A. H., Ho, Q. D., Truong, Q. T., Le, O. K., & Nguyen, L. H. P. (2021). Dumbbell configuration of silicon adatom defects on silicene nanoribbons. *Scientific Reports*, *11*(1), 14374. https://doi.org/10.1038/s41598-021-93465-5

Khoeini, F., & Jafarkhani, Z. (2019). Tunable spin transport and quantum phase transitions in silicene materials and superlattices. *Journal of Materials Science, 54*(23), 14483–14494. https://link.springer.com/article/10.1007%2Fs10853-019-03928-4

Kim, K., Coh, S., Kisielowski, C., Crommie, M. F., Louie, S. G., Cohen, M. L., & Zettl, A. (2013). Atomically perfect torn graphene edges and their reversible reconstruction. *Nature Communications*, *4*(1), 2723. https://doi.org/10.1038/ncomms3723

Le, M.-Q., & Nguyen, D.-T. (2015). The role of defects in the tensile properties of silicene. *Applied Physics A*, *118*(4), 1437–1445. https://doi.org/10.1007/s00339-014-8904-3

Li, S., Wu, Y., Tu, Y., Wang, Y., Jiang, T., Liu, W., & Zhao, Y. (2015). Defects in silicene: Vacancy clusters, extended line defects and di-adatoms. *Scientific Reports*, *5*(1), 7881. https://doi.org/10.1038/srep07881

Manjanath, A., & Singh, A. K. (2014). Low formation energy and kinetic barrier of Stone–Wales defect in infinite and finite silicene. *Chemical Physics Letters*, *592*, 52–55. https://doi.org/10.1016/j.cplett.2013.12.010

Molle, A., Grazianetti, C., Tao, L., Taneja, D., Alam, Md. H., & Akinwande, D. (2018). Silicene, silicene derivatives, and their device applications. *Chemical Society Reviews*, *47*(16), 6370. https://doi.org/10.1039/C8CS00338F

Mortazavi, B., & Ahzi, S. (2013). Thermal conductivity and tensile response of defective graphene: A molecular dynamics study. *Carbon*, *63*, 460–470. https://doi.org/10.1016/j.carbon.2013.07.017

Ngo, V.-C., Nguyen, T.-K.-Q., Pham, N.-H.-H., Pham, T.-H., Phan, T.-K.-L., Do, V.-N., & Vu, T.-T. (2023). Effects of divacancies on the electronic properties of zigzag-edge buckling silicene nanoribbons. *Physica B: Condensed Matter*, *670*, 415390. https://doi.org/10.1016/j.physb.2023.415390

Nguyen, T.-K.-Q., Pham, N.-H.-H., Kim, L.-P. T., Vu, T.-T., & Tran, V.-T. (2021). Effect of electric fields on the electronic and thermoelectric properties of zigzag buckling silicene nanoribbons. *Advances in Natural Sciences: Nanoscience and Nanotechnology*, *12*(3), 035002. https://iopscience.iop.org/article/10.1088/2043-6262/ac204b/meta

Novoselov, K. S., Geim, A. K., Morozov, S. V., Jiang, D., Zhang, Y., Dubonos, S. V., Grigorieva, I. V., & Firsov, A. A. (2004). Electric field effect in atomically thin carbon films. *Science*, *306*(5696), 666–669. https://doi.org/10.1126/science.1102896

Novoselov, K. S., Geim, A. K., Morozov, S. V., Jiang, D., Katsnelson, M. I., Grigorieva, I. V., & Firsov, A. A. (2005). Two-dimensional gas of massless Dirac fermions in graphene. *Nature*, *438*, 197–200. https://doi.org/10.1038/nature04233

Peng, Q., Wen, X., & De, S. (2013). Mechanical stabilities of silicene. *RSC Advances*, *3*(33), 13772–13781. https://doi.org/10.1039/C3RA41347K

Peng, W., Liu, P., Zhang, X., Peng, J., Gu, Y., Dong, X., Ma, Z., Liu, P., & Shen, J. (2020). Multi-functional zwitterionic coating for silicone-based biomedical devices. *Chemical Engineering Journal*, *398*, 125663. https://doi.org/10.1016/j.cej.2020.125663

Piraux, B., Galstyan, A., Popov, Y. V., Mota-Furtado, F., & O'Mahony, P. F. (2021). Iterative treatment of the Coulomb potential in laser–atom interactions. *The European Physical Journal D*, *75*(7), 196. https://doi.org/10.1140/epjd/s10053021-00174-9

Sahin, H., Cahangirov, S., Topsakal, M., Bekaroglu, E., Akturk, E., Senger, R. T., & Ciraci, S. (2009). Monolayer honeycomb structures of group-IV elements and III-V binary compounds: First-principles calculations. *Physical Review B*, *80*(15), 155453. https://doi.org/10.1103/PhysRevB.80.155453

Sahin, H., Sivek, J., Li, S., Partoens, B., & Peeters, F. M. (2013). Stone-Wales defects in silicene: Formation, stability, and reactivity of defect sites. *Physical Review B*, *88*(4), 045434. https://doi.org/10.1103/PhysRevB.88.045434

Shirodkar, S. N., & Waghmare, U. V. (2012). Electronic and vibrational signatures of Stone-Wales defects in graphene: First-principles analysis. *Physical Review B*, *86*(16), 165401. https://doi.org/10.1103/PhysRevB.86.165401

Sivek, J., Sahin, H., Partoens, B., & Peeters, F. M. (2013). Adsorption and absorption of boron, nitrogen, aluminum, and phosphorus on silicene: Stability and electronic and phonon properties. *Physical Review B*, *87*(8), 085444. https://doi.org/10.1103/PhysRevB.87.085444

Vogt, P., De Padova, P., Quaresima, C., Avila, J., Frantzeskakis, E., Asensio, M. C., Resta, A., Ealet, B, & Lay, G. L. (2012). Silicene: Compelling experimental evidence for graphenelike two-dimensional silicon. *Physical Review Letters*, *108*(15), 155501. https://doi.org/10.1103/PhysRevLett.108.155501

Zhang, P., Li, X. D., Hu, C. H., Wu, S. Q., & Zhu, Z. Z. (2012). First-principles studies of the hydrogenation effects in silicene sheets. *Physics Letters A*, *376*(14), 1230–1233. https://doi.org/10.1016/j.physleta.2012.02.030

Zhang, X., Zhang, D., Xie, F., Zheng, X., Wang, H., & Long, M. (2017). First-principles study on the magnetic and electronic properties of Al or P doped armchair silicene nanoribbons. *Physics Letters A*, *381*(25–26), 2097–2102. https://doi.org/10.1016/j.physleta.2017.04.030

Zhu, J., & Schwingenschlögl, U. (2016). Silicene for Na-ion battery applications. *2D Materials*, *3*(3), 035012. https://iopscience.iop.org/article/10.1088/2053-1583/3/3/035012